Letter

Partial magnetic order in kagome spin ice

Eric C. Andrade [1] and Matthias Vojta[2]

[1]*Instituto de Física, Universidade de São Paulo, C.P. 66318, 05315-970 São Paulo, São Paulo, Brazil*
[2]*Institut für Theoretische Physik and Würzburg-Dresden Cluster of Excellence ct.qmat, Technische Universität Dresden,
01062 Dresden, Germany*

Motivated by the observation of partial magnetic order in kagome-based magnets, we study the classical kagome Ising antiferromagnet, known as kagome spin ice, including further-neighbor interactions at zero and finite temperature. While the nearest-neighbor model displays an extensive ground-state degeneracy, various symmetry-breaking states can appear upon including additional couplings. Among these, peculiar partially ordered states have been proposed. We present results from large-scale Monte Carlo simulations, establishing that such partial order is stabilized by third-neighbor couplings along the hexagon diagonals. We show that these states arise due to the emergence of one-dimensional chains in an entirely frustrated environment, and that they are stable with respect to further couplings. We discuss their finite-temperature properties in detail, highlight the magnetic states' peculiarities depending on the diagonal couplings' sign, and suggest observing these states using thermodynamic probes.

Highly frustrated magnets constitute a prime territory in the quest for novel phases of matter. Those include nontrivial forms of order and disorder, such as quantum spin liquids, spin nematics, as well as skyrmions and other topological magnetic textures [1–6]. A fascinating class of states is that with partial magnetic order, where a fraction of the magnetic moments display symmetry-breaking long-range order while another fraction remains fluctuating to low temperatures. Such partially ordered (or, equivalently, partially disordered) states have been reported for a few compounds, among them the heavy-fermion metals CePdAl [7] and UNi_4B [8], as well as the insulating magnets Sr_2YRuO_6 [9], $Gd_2Ti_2O_7$ [10], $LiZn_2Mo_3O_8$ [11], HoAgGe [12], and $Fe_4Si_2Sn_7O_{16}$ [13,14].

Partially ordered states have also appeared in various theoretical models, including Ising models [15–19], classical vector-spin models at finite T [10,20], quantum Heisenberg models [21,22], and Kondo models with partial screening [23]. In all cases, the critical ingredient is that the network of the ordered moments does not exert any mean field on the remaining fluctuating moments. The latter fluctuating magnetic moments effectively remove a fraction of the frustrated bonds while retaining entropy, thus lowering the free energy. However, in such a situation, order by disorder [24–26] would still be possible, and the precise mechanism preventing a complete ordering is specific for each case. Notably, conclusive links between theory and experiment are rare [10], and further well-understood examples are paramount to building a general scenario.

Kagome ice [18], referring to spins on the two-dimensional kagome lattice with infinite local Ising anisotropy, belongs to the class of frustrated Ising models [12]. In its simplest version, it features a macroscopic ground-state degeneracy and a variety of order-by-disorder phases, resulting in a nontrivial temperature evolution of the magnetic states [27–30]. A partially ordered phase has been proposed early on to occur in

a model supplemented by second-neighbor interactions [18], and this proposal has been discussed *vis-à-vis* experimental data [14]. In this Letter, we revisit the issue of partial order in kagome ice [12]. Utilizing large-scale Monte Carlo (MC) simulations, we show the previous proposal [18] to be incorrect. At the same time, we identify a distinct parameter regime where partial order is indeed stabilized at low T—this is facilitated by including a third-neighbor coupling along the diagonals of the hexagons. The spins connected via this extra coupling form one-dimensional chains coupled by ice rules. Such an exquisite arrangement leads to intense frustration and dimensional reduction because one out of three chains experiences a vanishing mean field and is entropically disordered at any finite T. The resulting model for ferromagnetic diagonal coupling displays two thermal phase transitions of Kosterlitz-Thouless (KT) type, with partial order emerging below the lower transition. We also investigate this model's antiferromagnetic cousin, finding a single transition and partial order at low T. We suggest the latter model being of relevance to $Fe_4Si_2Sn_7O_{16}$.

Model. The kagome ice model [18] describes spins $S_i = \sigma_i \hat{e}_i$ on the vertices of the kagome lattice in the limit of infinite Ising anisotropy. The local axes $\hat{e}_i$ connect the centers of adjacent triangles and point out of the upward triangles, and the $\sigma_i = \pm 1$ encode the Ising degree of freedom [see Fig. 1(a)]. In terms of the Ising degrees of freedom, the Hamiltonian reads

$$\mathcal{H} = J_1 \sum_{\langle i,j \rangle} \sigma_i \sigma_j + J_2 \sum_{\langle\langle i,j \rangle\rangle} \sigma_i \sigma_j - J_d \sum_{\langle\langle\langle i,j \rangle\rangle\rangle} \sigma_i \sigma_j$$
$$- J_3 \sum_{\langle\langle\langle i,j \rangle\rangle\rangle} \sigma_i \sigma_j, \tag{1}$$

where $J_{1,2,3,d}$ denotes first-neighbor, second-neighbor, third-neighbor across a site, and third-neighbor diagonal couplings, respectively, as in Fig. 1(a). The signs in Eq. (1) account
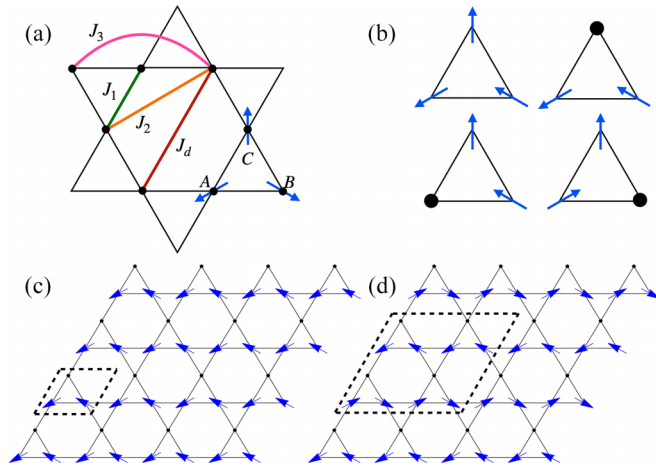
FIG. 1. (a) Kagome lattice and its three sublattices, dubbed A, B, and C. For each sublattice, we define the local axes $\hat{e}_i$ as shown by the arrows. The exchange couplings are J_1, J_2, J_3, and J_d between first, second, third neighbors across a site, and diagonal spins, respectively. (b) Local spin configuration satisfying the ice rules, alongside three local configurations for the partially disordered state, all shown in the global frame. (c), (d) Partially disordered states, in the global frame, as favored by (c) $J_d > 0$ and (d) $J_d < 0$. The black dots indicate the disordered sites, while the dashed lines show the magnetic unit cell.

for the relative orientation of the local Ising axes, such that $J_{1,2,3,d} > 0$ corresponds to ferromagnetic exchange couplings in the global frame. A dominant J_1 imposes ice rules at low energy such that we have two spins in and one out or vice versa for each triangle [Fig. 1(b)]. We also note that, in applied fields, the saturated magnetization can be parallel to any of the three local axes, corresponding to a Z_6 symmetry.

Overview of parameter regimes. Before describing our results for the model in Eq. (1), we quickly summarize those from the literature [17,18,27–30]. For ferromagnetic $J_1 > 0$ and $J_{2,3,d} = 0$, Eq. (1) displays an extensive manifold of degenerate ground states. For $J_2 < 0$ and $J_{3,d} = 0$, this macroscopic degeneracy is completely lifted, resulting in an ordered $\sqrt{3} \times \sqrt{3}$ state [28,29]. For $J_2 > 0$, Wills *et al.* [18] proposed a partially ordered phase to exist [Fig. 1(c)]; our results below indicate that this proposal is incorrect. In contrast, when all couplings are antiferromagnetic, the model displays macroscopically degenerate ground-state phases [30], hence a finite residual entropy survives for $J_2 > 0$ and $J_{3,d} < 0$ in extended regions of the phase diagram, showing that further couplings do not always select ordered ground states out of the disordered spin-ice manifold [30].

To stabilize partial order as in Figs. 1(c) and 1(d), it appears plausible to introduce a diagonal coupling J_d while setting $J_{2,3} = 0$. This is easiest seen in the limit $|J_d| \gg J_1$: For $J_1 = 0$, the system decomposes into three Ising chains, which remain disordered at any finite T. A finite coupling J_1 locally imposes the ice rules and couples the chains but leaves a degeneracy. We then expect the partially ordered states in Figs. 1(c) and 1(d) to emerge for $J_1 > 0$, $J_d \neq 0$, and $J_{2,3} = 0$, by combining the effects of the spin-ice rules and the strong thermal fluctuations in spin chains. This model has not been studied extensively; this is the main target of this Letter.

MC simulations. We study Eq. (1) using classical MC simulations on lattices of linear size L, with three sites per unit cell [Fig. 1(a)], and periodic boundary conditions. The total number of sites is $N = 3L^2$, and we consider $L = 12$ up to $L = 72$. We perform equilibrium MC simulations using single-site Metropolis updates combined with the parallel tempering method [31]. Due to its highly frustrated nature, this system may not reach equilibrium at low T sometimes, even for moderate system sizes. This, however, does not prevent us from extracting a general scenario for the thermodynamic behavior of Eq. (1).

To characterize the putative partially ordered phases, we compute the magnetization in the global frame for each up-triangle inside the magnetic unit cell. An average over all up-triangles in a given MC configuration returns a two-dimensional vector $\boldsymbol{m} = (m_x, m_y)$. We define $m = |\langle \boldsymbol{m} \rangle|$ where the brackets $\langle \cdots \rangle$ denote the MC average. According to Fig. 1(b), $m \rightarrow 1/\sqrt{3}$ in the partially ordered phases as $T \rightarrow 0$. It is useful to compute the histogram of the magnetization $P(m_x, m_y)$, which is expected to display peaks at $(m \cos \theta, m \sin \theta)$ with $\theta = \arctan(m_y/m_x) = n\pi/3$, $n = 0, 1, \ldots, 5$ for $T \rightarrow 0$, different from a fully ordered state [32]. We also compute the static spin structure factor, differentiating between the two partially ordered states, as they have different magnetic unit cells. Finally, we calculate the Edwards-Anderson order parameter, $q = \langle \sum_i \sigma_i^{(1)} \sigma_i^{(2)} \rangle / N$ where (1,2) are replica indices. q reflects the long-time autocorrelation function of a spin in an MC simulation [33]. Therefore, $q = 0$ in the paramagnetic phase while $|q| \rightarrow 1$ in a state with all spins frozen. In the partially ordered states, we expect $|q| \rightarrow 4/9$ instead [32].

Partially ordered ferromagnet. As motivated above, we focus on a model with positive J_1 and J_d, while $J_{2,3} = 0$, to stabilize the partially ordered stripe configuration in Fig. 1(c). Thermodynamic data for $J_d/J_1 = 0.4$ are shown in Fig. 2. The specific heat shows two peaks, with a weak dependence on system size, which we identify as phase transitions at T_{c1} and T_{c2} [Fig. 2(a)]. Both peak locations scale with J_d and tend to merge as J_d increases further. Also, for small J_d, there is a bump in the specific heat at $T/J_1 \approx 1.8$, signaling the onset of ice rules [18,32]. The magnetization approaches $1/\sqrt{3}$ as $T \rightarrow 0$, strongly hinting that we enter the partially ordered phase with $1/3$ of the spins fluctuating [Fig. 2(b)]. Following Refs. [17,28,29], we interpret the results as follows: Upon cooling from high T, we enter a critical intermediate phase with power-law correlations characterized by $m \sim L^{-\eta/2}$. Indeed, power-law fits to the magnetization data in Fig. 2(c) represent the data well and yield the exponents shown in Fig. 2(d). The critical phase expected for the six-state clock model is characterized by $\eta(T_{c1}) = 1/4$ and $\eta(T_{c2}) = 1/9$ [34–36], which enables us to determine $T_{c1,2}$ more accurately. The KT character of the two transitions is also compatible with the weak dependence of $C(T)$ on system size. We finally enter the partially ordered phase for $T < T_{c2}$. Integrating the specific heat, we detect no extensive zero-point entropy, indicating that the residual fluctuations are correlated and the ground state is unique (up to discrete symmetries). This is consistent with the proposed partially ordered state whose entropy density vanishes as $T \rightarrow 0$ because the spin correlation length along the chains diverges, $\xi_{\text{chain}} \gg L$.
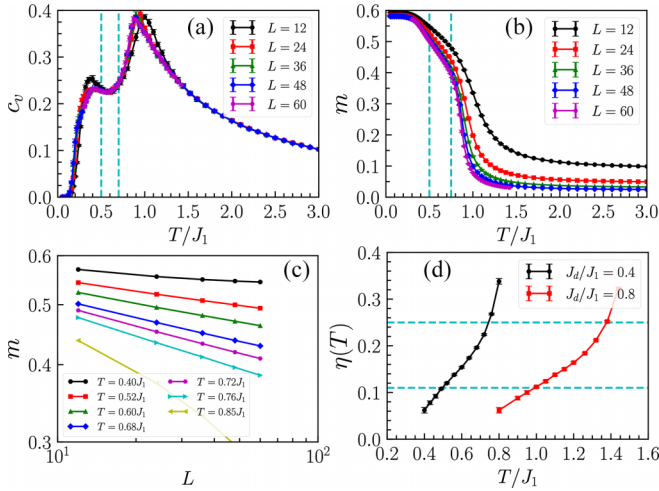
FIG. 2. MC results for the kagome ice model with ferromagnetic $J_d/J_1 = 0.4$. (a) Specific heat $C(T)$ for different linear system sizes L; the vertical dashed lines show the extent of the critical region (see text). (b), (c) Magnetization for the up-triangles in the global frame plotted as (b) $m(T)$ and (c) $m(L)$. (d) Magnetization exponent $\eta(T)$ from $m \sim L^{-\eta/2}$, characterizing the critical region. Here, we also show data for $J_d/J_1 = 0.8$.

The histogram of the global magnetization $P(m_x, m_y)$ is shown in Fig. 3. In the high-temperature paramagnet, it is featureless and centered at $m = 0$. The intermediate critical phase displays a ring-shaped structure, i.e., emergent U(1) symmetry [37]. For low T, it has the six-peak structure expected for the partially ordered phase, reflecting the emergent clock anisotropy of the model. Finally, the Edwards-Anderson order parameter reaches the expected value of 4/9 at low T [32].

Strain pinning of partial order. To corroborate the presence of partial order, we study the system in the presence of spatial anisotropy in J_d: For one of the three diagonal directions, we set $J_d \to J_d(1 - \Delta)$. For $\Delta > 0$, the partial order should be pinned along this direction because of the weaker couplings. Numerical results are shown in Fig. 4.

The spin correlations in Fig. 4(a) reflect order emerging along the strong bond direction but decaying correlations along the weak direction. We expect these spins to behave as ferromagnetic Ising chains, with a correlation length ξ_{chain} diverging as $T \to 0$. This picture perfectly matches our results for the Edwards-Anderson order parameter [Fig. 4(b)]. As
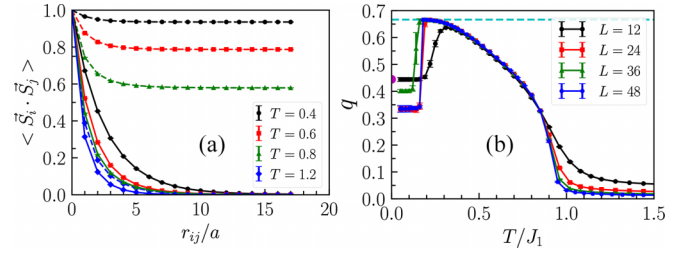
FIG. 4. MC results for the kagome ice model with spatially anisotropic J_d, using $J_d/J_1 = 0.4$ and $\Delta = 0.2$. (a) Spin-spin correlation function (in the global frame) for spins along the hexagon diagonals as a function of distance, with solid (dashed) lines showing correlations along the weak (strong) bonds. (b) Edwards-Anderson order parameter $q(T)$. The horizontal dashed line indicates $q = 2/3$ and the red dot $q = 4/9$.

long as ξ_{chain} is smaller than the system size L, we have $q \to 2/3$, indicating that 1/3 of the spins fluctuate. At low T when $\xi_{\text{chain}} > L$, there is a sudden drop in q, and it becomes equally probable for any of the three chains to fluctuate. For $L = 12$, we recover the uniform result $q \to 4/9$. For larger system sizes, however, the runs do not reach equilibrium in this regime, as the magnetic states become markedly distinct above and below the drop in q, rendering the parallel tempering algorithm inefficient. We have also computed $P(m_x, m_y)$ for the case of anisotropic couplings, displaying only two peaks, corresponding to the selection of a single domain with the disordered chains running along the weaker bonds [32].

These results establish partial order in the kagome ice model with $J_{1,d} > 0$. For $0 < T < T_{c2}$, we see that 2/3 of the spins show ferromagnetic long-range order, and the remaining 1/3 form a set of effectively decoupled Ising chains which only order at $T = 0$. The state below T_{c2} thus spontaneously breaks a spatial Z_3 symmetry by selecting a chain direction.

Partially ordered antiferromagnet. Motivated by the results for $J_d > 0$, we now study the model with $J_d < 0$, searching for the partially ordered antiferromagnet in Fig. 1(d), which is likely of experimental relevance for $Fe_4Si_2Sn_7O_{16}$.

As shown in Fig. 5(a), the specific heat now shows a single peak whose temperature grows with J_d, consistent with a single phase transition. The magnetization, per up-triangle in the unit cell, approaches $1/\sqrt{3}$ as $T \to 0$ [Fig. 5(b)], as expected for partial order.
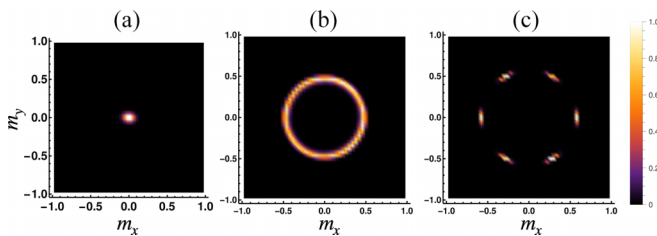

FIG. 3. Magnetization distribution $P(m_x, m_y)$ obtained for $L = 48$ and $J_d/J_1 = 0.4$. (a) $T/J_1 = 1.2$, (b) $T/J_1 = 0.6$, and (c) $T/J_1 = 0.3$.
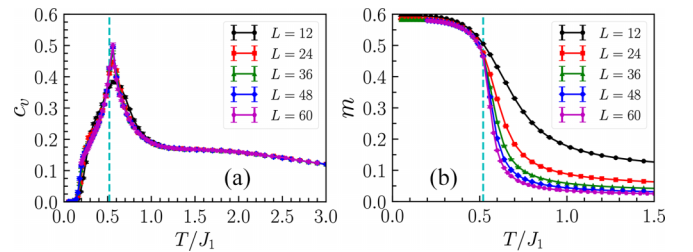

FIG. 5. MC results for the kagome ice model with antiferromagnetic $J_d/J_1 = -0.4$. (a) Specific heat $C(T)$ for different system sizes. The dashed line estimates T_c. (b) Magnetization $m(T)$ [32].
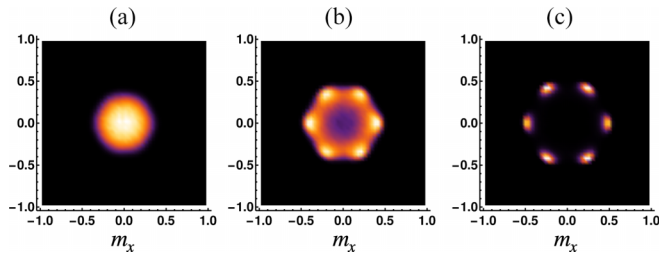
FIG. 6. Magnetization distribution $P(m_x, m_y)$ obtained for $L = 24$ and $J_2/J_1 = -0.4$. (a) $T/J_1 = 0.6$, (b) $T/J_1 = 0.56$, and (c) $T/J_1 = 0.52$. The color scale is the same as in Fig. 3.

FIG. 8. Magnetization distribution $P(m_x, m_y)$ obtained for $L = 48$ and $J_2/J_1 = 0.1$. (a) $T/J_1 = 0.2$, (b) $T/J_1 = 0.1$, and (c) $T/J_1 = 0.05$. The color scale is defined in Fig. 3.

$P(m_x, m_y)$ displays the expected six-peak structure at low T (Fig. 6). We find no evidence for a ring-shaped $P(m_x, m_y)$, consistent with the absence of a critical phase for all investigated values of J_d [32]. We believe this difference between the ferromagnetic and antiferromagnetic cases is rooted in the different magnetic unit cells [Figs. 1(c) and 1(d) and Figs. S1(a) and S1(b) [32]]. For $J_d < 0$, a given state and its time-reversal equivalent are related by a simple translation. This suggests an emerging three-state clock anisotropy and a single transition [34].

We have also studied the antiferromagnetic case in the presence of spatial anisotropy in J_d to pin the disordered spins' manifold. Numerical results are shown in the Supplemental Material [32], again consistent with a partial order, with 1/3 of the spin forming antiferromagnetic Ising chains, which only order at $T = 0$.

No partial order driven by J_2. We finally turn to the model initially proposed in Ref. [18] to show partial order, namely the model with $J_{3,d} = 0$ and ferromagnetic J_2 instead. Thermodynamic results are shown in Fig 7. For small J_2, we observe two broad peaks in $C(T)$, which tend to merge at larger J_2. Integrating $C(T)$, we find a finite residual entropy, consistent with this model displaying an extensive ground-state degeneracy [17,38,39]. A Pauling argument can estimate the entropy, considering that J_1 enforces ice rules on the original lattice whereas J_2 enforces ice rules on the respective kagome superlattices [32]. A more precise value of the residual entropy is $S_0 = 0.2853N$ [38], consistent with our data. This discussion implies that the two peaks in $C(T)$ correspond to crossovers where these ice rules are enforced by J_1 and J_2, respectively.
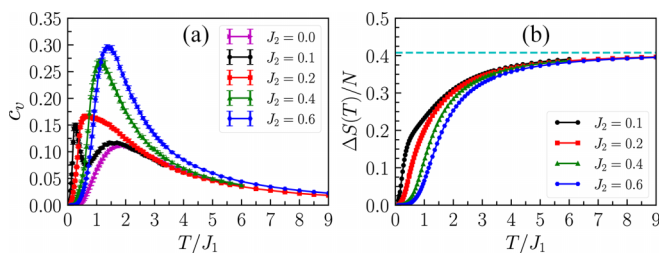
The magnetization data appear consistent with a KT transition in the limit $T \to 0$, as proposed in Ref. [17]. For $T < J_1$, we observe a power-law behavior $m \sim L^{-\eta/2}$, with $\eta \to 1/4$ as $T \to 0$ [32]. The absence of a finite-T transition is consistent with the finite residual entropy we identify in Fig. 7(b). More direct counterevidence concerning partial disorder comes from the histogram $P(m_x, m_y)$ in Fig. 8. Here, we see a continuous ring structure down to the lowest T, akin to the critical phase discussed above, with no sign of the six-peak structure.

We conclude that the model with finite J_2 (and $J_{3,d} = 0$) does not realize a state with partial order. Instead, its low-T phase is critical with power-law correlations, and the partially ordered state represents only one of the many possible low-T states of the model.

Summary. For variants of kagome spin ice, with first-neighbor and diagonal third-neighbor couplings, we have established the existence of partially ordered magnetic states where 1/3 of the spins continue to fluctuate down to $T \to 0$ in the background of either ferromagnetic or antiferromagnetic bulk order. The origin is intense frustration and dimensional reduction: The fluctuating spins form effective Ising chains, which experience no mean field and are entropically disordered at $T > 0$.

This peculiar state is robust with respect to additional (weak) second-neighbor coupling J_2 and a third-neighbor coupling J_3 across a site [Fig. 1(a)]. Both perturbations cause no mean field on the disordered sites, thus preserving the partially disordered state. However, J_3 locks neighboring disordered chains into a long-range ordered state, resulting in a weakly ordered state at low T [32].

Our findings are likely relevant to $Fe_4Si_2Sn_7O_{16}$, and we propose to combine specific-heat measurements with local probes to disentangle the energy scales at which the ice rules are imposed and the partial order emerges. Moreover, measurements under uniaxial strain, as simulated here, will be key to nail down the one-dimensional nature of the partially ordered state. Extending the present theory beyond the limit of infinite Ising anisotropy and in the presence of a magnetic field is the subject of ongoing work.

FIG. 7. MC results for the kagome ice model with finite J_2, but $J_d = 0$. (a) Specific heat $C(T)$ and (b) entropy difference $\Delta S(T) = S(T) - S_0$ for different values of J_2 and system size $L = 36$. The dashed line in (b) corresponds to $\ln 2 - S_0$ with the exact value of S_0 from Ref. [38].
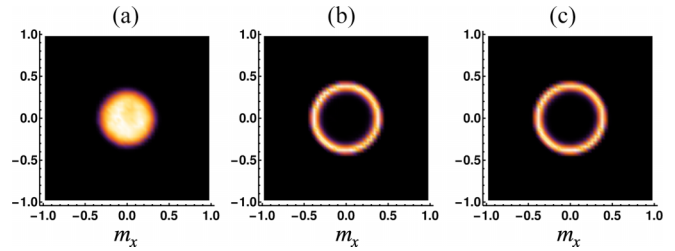
[1] C. Lacroix, P. Mendels, and F. Mila, *Introduction to Frustrated Magnetism: Materials, Experiments, Theory*, Springer Series in Solid-State Sciences (Springer, Berlin, 2011).

[2] C. Castelnovo, R. Moessner, and S. Sondhi, Spin ice, fractionalization, and topological order, Annu. Rev. Condens. Matter Phys. **3**, 35 (2012).

[3] A. Fert, N. Reyren, and V. Cros, Magnetic skyrmions: Advances in physics and potential applications, Nat. Rev. Mater. **2**, 17031 (2017).

[4] M. Vojta, Frustration and quantum criticality, Rep. Prog. Phys. **81**, 064501 (2018).

[5] R. M. Fernandes, P. P. Orth, and J. Schmalian, Intertwined vestigial order in quantum materials: Nematicity and beyond, Annu. Rev. Condens. Matter Phys. **10**, 133 (2019).

[6] S. Sachdev, *Quantum Phases of Matter* (Cambridge University Press, Cambridge, UK, 2023).

[7] A. Oyamada, S. Maegawa, M. Nishiyama, H. Kitazawa, and Y. Isikawa, Ordering mechanism and spin fluctuations in a geometrically frustrated heavy-fermion antiferromagnet on the Kagome-like lattice CePdAl: A ^{27}Al NMR study, Phys. Rev. B **77**, 064432 (2008).

[8] R. Movshovich, M. Jaime, S. Mentink, A. A. Menovsky, and J. A. Mydosh, Second low-temperature phase transition in frustrated UNi$_4$B, Phys. Rev. Lett. **83**, 2065 (1999).

[9] E. Granado, J. W. Lynn, R. F. Jardim, and M. S. Torikachvili, Two-dimensional magnetic correlations and partial long-range order in geometrically frustrated Sr$_2$YRuO$_6$, Phys. Rev. Lett. **110**, 017202 (2013).

[10] B. Javanparast, Z. Hao, M. Enjalran, and M. J. P. Gingras, Fluctuation-driven selection at criticality in a frustrated magnetic system: The case of multiple-**k** partial order on the pyrochlore lattice, Phys. Rev. Lett. **114**, 130601 (2015).

[11] J. P. Sheckelton, J. R. Neilson, D. G. Soltan, and T. M. McQueen, Possible valence-bond condensation in the frustrated cluster magnet LiZn$_2$Mo$_3$O$_8$, Nat. Mater. **11**, 493 (2012).

[12] K. Zhao, H. Deng, H. Chen, K. A. Ross, V. Petříček, G. Günther, M. Russina, V. Hutanu, and P. Gegenwart, Realization of the kagome spin ice state in a frustrated intermetallic compound, Science **367**, 1218 (2020).

[13] C. D. Ling, M. C. Allison, S. Schmid, M. Avdeev, J. S. Gardner, C.-W. Wang, D. H. Ryan, M. Zbiri, and T. Söhnel, Striped magnetic ground state of the kagome lattice in Fe$_4$Si$_2$Sn$_7$O$_{16}$, Phys. Rev. B **96**, 180410(R) (2017).

[14] S. Dengre, R. Sarkar, L. Opherden, T. Herrmannsdörfer, M. Allison, T. Söhnel, C. D. Ling, J. S. Gardner, and H.-H. Klauss, Magnetic anisotropy and spin dynamics in the kagome magnet Fe$_4$Si$_2$Sn$_7$O$_{16}$: NMR and magnetic susceptibility study on oriented powder, Phys. Rev. B **103**, 064425 (2021).

[15] M. Mekata, Antiferro-ferrimagnetic transition in triangular Ising lattice, J. Phys. Soc. Jpn. **42**, 76 (1977).

[16] D. Blankschtein, M. Ma, A. N. Berker, G. S. Grest, and C. M. Soukoulis, Orderings of a stacked frustrated triangular system in three dimensions, Phys. Rev. B **29**, 5250(R) (1984).

[17] T. Takagi and M. Mekata, Magnetic ordering of Ising spins on kagome lattice with the 1st and the 2nd neighbor interactions, J. Phys. Soc. Jpn. **62**, 3943 (1993).

[18] A. S. Wills, R. Ballou, and C. Lacroix, Model of localized highly frustrated ferromagnetism: The kagome spin ice, Phys. Rev. B **66**, 144407 (2002).

[19] H. Ishizuka and Y. Motome, Partial disorder in an Ising-spin Kondo lattice model on a triangular lattice, Phys. Rev. Lett. **108**, 257205 (2012).

[20] C. Santamaria and H. T. Diep, Evidence of partial disorder in a frustrated Heisenberg spin system, J. Appl. Phys. **81**, 5276 (1997).

[21] M. G. Gonzalez, F. T. Lisandrini, G. G. Blesio, A. E. Trumper, C. J. Gazza, and L. O. Manuel, Correlated partial disorder in a weakly frustrated quantum antiferromagnet, Phys. Rev. Lett. **122**, 017201 (2019).

[22] U. F. P. Seifert and M. Vojta, Theory of partial quantum disorder in the stuffed honeycomb Heisenberg antiferromagnet, Phys. Rev. B **99**, 155156 (2019).

[23] Y. Motome, K. Nakamikawa, Y. Yamaji, and M. Udagawa, Partial Kondo screening in frustrated Kondo lattice systems, Phys. Rev. Lett. **105**, 036403 (2010).

[24] J. Villain, R. Bidaux, J.-P. Carton, and R. Conte, Order as an effect of disorder, J. Phys. (France) **41**, 1263 (1980).

[25] E. F. Shender, Antiferromagnetic garnets with fluctuationally interacting sublattices, Zh. Eksp. Teor. Fiz. **83**, 326 (1982) [Sov. Phys. JETP **56**, 178 (1982)].

[26] C. L. Henley, Ordering due to disorder in a frustrated vector antiferromagnet, Phys. Rev. Lett. **62**, 2056 (1989).

[27] G. Möller and R. Moessner, Magnetic multipole analysis of kagome and artificial spin-ice dipolar arrays, Phys. Rev. B **80**, 140409(R) (2009).

[28] G.-W. Chern, P. Mellado, and O. Tchernyshyov, Two-stage ordering of spins in dipolar spin ice on the kagome lattice, Phys. Rev. Lett. **106**, 207202 (2011).

[29] G.-W. Chern and O. Tchernyshyov, Magnetic charge and ordering in kagome spin ice, Philos. Trans. R. Soc. London, Ser. A **370**, 5718 (2012).

[30] J. Colbois, B. Vanhecke, L. Vanderstraeten, A. Smerald, F. Verstraete, and F. Mila, Partial lifting of degeneracy in the J_1-J_2-J_3 Ising antiferromagnet on the kagome lattice, Phys. Rev. B **106**, 174403 (2022).

[31] M. Newman and G. Barkema, *Monte Carlo Methods in Statistical Physics* (Clarendon Press, Oxford, UK, 1999).

[32] See Supplemental Material at http://link.aps.org/supplemental/10.1103/PhysRevB.109.L241102 for further details of the characterization of the partial orders in the Monte Carlo simulations and additional results and discussions, which includes Refs. [40,41].

[33] L. W. Lee and A. P. Young, Large-scale Monte Carlo simulations of the isotropic three-dimensional Heisenberg spin glass, Phys. Rev. B **76**, 024405 (2007).

[34] J. V. José, L. P. Kadanoff, S. Kirkpatrick, and D. R. Nelson, Renormalization, vortices, and symmetry-breaking

perturbations in the two-dimensional planar model, Phys. Rev. B **16**, 1217 (1977).

[35] C. C. Price and N. B. Perkins, Critical properties of the Kitaev-Heisenberg model, Phys. Rev. Lett. **109**, 187201 (2012).

[36] C. Price and N. B. Perkins, Finite-temperature phase diagram of the classical Kitaev-Heisenberg model, Phys. Rev. B **88**, 024410 (2013).

[37] J. Lou, A. W. Sandvik, and L. Balents, Emergence of U(1) symmetry in the 3D XY model with Z_q anisotropy, Phys. Rev. Lett. **99**, 207203 (2007).

[38] J. Colbois, K. Hofhuis, Z. Luo, X. Wang, A. Hrabec, L. J. Heyderman, and F. Mila, Artificial out-of-plane Ising antiferromagnet on the kagome lattice with very small farther-neighbor couplings, Phys. Rev. B **104**, 024418 (2021).

[39] J. Hamp, R. Moessner, and C. Castelnovo, Supercooling and fragile glassiness in a dipolar kagome Ising magnet, Phys. Rev. B **98**, 144439 (2018).

[40] L. Messio, C. Lhuillier, and G. Misguich, Lattice symmetries and regular magnetic orders in classical frustrated antiferromagnets, Phys. Rev. B **83**, 184401 (2011).

[41] F. Oliviero, J. A. Sobral, E. C. Andrade, and R. G. Pereira, Noncoplanar magnetic orders and gapless chiral spin liquid on the kagome lattice with staggered scalar spin chirality, SciPost Phys. **13**, 050 (2022).